Synergistic Effects of Benzotriazole and Copper Ions on the Electrochemical Impedance Spectroscopy and Corrosion Behavior of Iron in Sulfuric Acid

S. Y. Sayed, M. S. El-Deab, B. E. El-Anadouli, and B. G. Ateya*

Chemistry Department, Faculty of Science, Cairo University, Cairo, Egypt

Received: February 9, 2003; In Final Form: April 14, 2003

Benzotriazole (BTAH) and copper ions exhibit synergistic effects on the electrochemical impedance spectroscopy and corrosion behavior of iron in sulfuric acid. The presence of submicro- and micromolar amounts of Cu^{2+} ions along with millimolar amounts of BTAH caused order of magnitude increases in the polarization resistance of the iron/acid interface, above those caused by either BTAH or Cu^{2+} ions (which is equivalent to order of magnitude decreases in the corrosion rate). This was accompanied by a significant decrease in the capacity of the electrical double layer of the interface, which also showed synergistic effects. The results are interpreted in terms of the deposition, on the iron surface, of a protective film composed of a polymeric complex formed from copper ions and adsorbed BTAH that is believed to be of the form $[Cu(I)BTA]_n$. This film inhibits the cathodic partial (hydrogen evolution) reaction, which is the rate-determining step (rds) and hence the overall corrosion reaction. An increase in the concentration of either Cu^{2+} or BTAH enhances this synergistic effect. However, there is a critical concentration of copper ions (5×10^{-6} M) beyond which further increase decreases the magnitude of the synergistic effect. This is attributed to deposition of metallic copper on the iron surface at higher concentrations of Cu^{2+} ions, which promotes the rds and hence the overall corrosion reaction. The results are supported by measurements of polarization curves and mass loss under various conditions.

Introduction

Benzotriazole (BTAH) has long been known as an efficient inhibitor for the corrosion of copper and its alloys.[1−10] It has also been tested on other metals, for example, Zn,[11−13] Al,[14] Co,[15] Ni[16], and various steels.[16−24] It was found to be less efficient than in the case of copper and its alloys. Two mechanisms have been proposed to account for the high inhibiting efficiency of BTAH against the corrosion of copper. The first attributes it to the adsorption of benzotriazole on the copper surface [3,25−34], that is

$$BTAH_{(aq)} + Cu \leftrightarrow BTAH{:}Cu \quad (1)$$

where BTAH:Cu refers to BTAH adsorbed on the copper surface. The adsorption of BTAH on copper substrates has been studied in aqueous media[25−31] and in ultrahigh vacuum.[3,32−34] It has been shown[3,28,30,31] that BTAH is attached to the (single as well as polycrystalline) copper substrate via a pair of triazole nitrogens with a tilted (or vertical) orientation. The second mechanism postulates the formation of a polymeric complex of Cu(I)BTA,[28−31,34−41] that is

$$n Cu^{+} + n BTAH \rightarrow [Cu(I)BTA]_n + n H^{+} \quad (2)$$

It has been amply confirmed that the remarkable inhibiting efficiency of BTAH (as high as 99+%) against the corrosion of copper and its alloys is attributed to the formation of this Cu(I)BTA complex on the copper surface. The binding between Cu(I) and BTAH in the Cu(I)BTA complex has also been extensively studied,[35,42] where evidence has been presented which suggests that the Cu(I) ion is attached to the triazole nitrogens of two BTAH molecules in a bridging arrangement.

Youda et al.[43] have suggested that adsorption and complex formation are in equilibrium, that is

$$n(BTAH)_{(ads)} + n Cu \leftrightarrow [Cu(I)BTA]_n + n H^{+} + n e \quad (3)$$

Equation 3 requires that increasing the pH value, inhibitor concentration, and potential in the noble direction favor the formation of the complex, while adsorption becomes favorable in acidic media, at lower inhibitor concentration and when the potential changes to more negative values. It has been shown[38,44] that the efficiency of BTAH against the corrosion of copper is significantly higher in neutral than in acidic media.

In the above studies, the Cu(I)BTA complex was formed on copper substrates, that is, from indigenous copper ions which have been freshly generated from the surface of the copper substrate. On the other hand, BTAH shows lower inhibition efficiencies against the corrosion of metals other than copper and its alloys. This has tempted some authors to try to synthesize and study the efficiency of a Cu(I)BTA film on non-copper substrates. Brusic et al.[15] were able to form a thin film of Cu(I)BTA on cobalt, which exhibited a higher protection efficiency against the corrosion of cobalt than benzotriazole alone. Some authors[45] showed that Cu^{2+} ions and BTAH exhibited a synergistic inhibiting effect on the rate of hydrogen permeation within iron, whereas others showed a similar effect on the polarization curves of iron.[46]

The objective of this paper is to study the synergistic effects of copper ions and BTAH on the electrochemical impedance spectroscopy and the corrosion behavior of iron in sulfuric acid.

* Corresponding author bgateya@yahoo.com.

10.1021/jp034334x CCC: $25.00
Published on Web 05/14/2003

TABLE 1: Effects of the Concentrations of BTAH and Cu^{2+} Ions on the Impedance Parameters of Iron in 0.5 M H_2SO_4 at 30 °C[a]

electrolyte composition		R_p, ohm cm^2	C, $\mu F\ cm^{-2}$	E_{corr}, V vs Hg/Hg_2SO_4	% P
A	0.5 M H_2SO_4	6.7	324.0	−0.850	
Cu^{2+} ions without BTAH	+ 5×10^{-6} M Cu^{2+}	9.4	276.2	−0.851	28.72
Figure 2	+ 10^{-5}	7.1	317.9	−0.849	5.63
	+ 10^{-4}	7.3	312.0	−0.848	8.22
B	0.5 M H_2SO_4	6.7	324.0	−0.850	
BTAH without Cu^{2+}	+10^{-3} M BTAH	13.1	183.1	−0.845	48.85
Figure 4	+5×10^{-3}	16.5	165.8	−0.834	59.39
	+10^{-2}	30.5	89.0	−0.843	78.03
	+5×10^{-2}	442.0	58.9	−0.828	98.48
C	0.5 M H_2SO_4	6.7	324.0	−0.850	
constant BTAH + varying Cu^{2+}	+ [BTAH] = 5×10^{-3} M	16.5	165.8	−0.834	59.39
Figures 1, 9, and 10	+ 2×10^{-7} M Cu^{2+}	61.0	69.1	−0.847	89.02
	+ 10^{-6}	374.2	32.0	−0.854	98.21
	+ 5×10^{-6}	612.5	21.5	−0.858	98.91
	+ 10^{-5}	460.0	34.4	−0.863	98.54
	+10^{-4}	187.0	67.8	−0.855	96.42
D	0.5 M H_2SO_4	6.7	324.0	−0.850	
varying BTAH + constant Cu^{2+}	+ [Cu^{2+}] = 5×10^{-6} M	9.4	276.2	−0.851	28.72
Figure 3	+ 10^{-3} M [BTAH]	27.4	161.5	−0.845	75.55
	+ 5×10^{-3}	612.5	21.5	−0.858	98.91
	+ 10^{-2}	1041.0	19.9	−0.878	99.36
	+ 5×10^{-2}	1606.0	19.6	−0.844	99.58
E	0.5 M H_2SO_4	6.7	324.0	−0.850	
varying BTAH + constant Cu^{2+}	+ [Cu^{2+}] = 10^{-5} M	7.1	307.9	−0.849	5.63
	+ 10^{-3}M [BTAH]	19.3	149.0	−0.846	65.28
	+ 5×10^{-3}	460.0	34.4	−0.863	98.54
	+ 5×10^{-2}	1434.2	25.4	−0.866	99.53
F	0.5 M H_2SO_4	6.7	324.0	−0.850	
varying BTAH + constant Cu^{2+}	+ [Cu^{2+}] = 10^{-4} M	7.3	312.0	−0.848	8.22
	+ 5×10^{-3} M [BTAH]	187.0	67.8	−0.855	96.42
	+10^{-2}	535.8	64.2	−0.863	98.75
	+ 5×10^{-2}	1209.1	58.0	−0.862	99.45

[a] R_p is the polarization resistance, C is the double-layer capacitance, E_{corr} is the free corrosion potential, and % P is the protection efficiency; see text and the inset in Figure 1B.

This is a subject of great industrial as well as academic significance. The overall corrosion reaction is represented by

$$Fe_{(s)} + 2H^{+}_{(aq)} = Fe^{+2}_{(aq)} + H_{2(g)} \quad (4)$$

This reaction is known to be composed of two partial reactions. The anodic partial reaction is

$$Fe_{(s)} \rightarrow Fe^{+2}_{(aq)} + 2e \quad (5)$$

and the cathodic partial reaction is

$$2H^{+}_{(aq)} + 2e \rightarrow H_{2(g)} \quad (6)$$

In this system the cathodic partial reaction is the rate-determining step (rds) in the overall corrosion reaction. We present below the results of a systematic study that includes measurements of electrochemical impedance spectroscopy (EIS), polarization curves, and weight loss.

Experimental Section

The iron used had the following composition in mass percent: 0.176 C, 0.132 Si, 0.776 Mn, 0.023 P, 0.020 S, and 98.8+ Fe. The specimens were polished on wet SiC paper (120, 1000, 1200), washed with distilled water, degreased in ethanol, and finally dried before testing. Electrochemical measurements were performed in a three-electrode cell, using an EG&G potentiostat (model 273A) and a lock-in amplifier (model 5210), operated with Corr 352 and EIS M398 software. The working electrode was fitted into glass tubing of appropriate internal diameter by epoxy resin, leaving a surface area of 0.5 cm^2 to contact the solution. A platinum wire was used as a counter electrode, and an Hg/Hg_2SO_4 was used as a reference electrode (its standard potential is 615 mV vs SHE). The electrolytes were prepared using analytical grade chemicals and triple-distilled water. The cell was kept at 30 ± 1 °C. The test solution was 0.5 M H_2SO_4 solution in the presence and in the absence of benzotriazole and/or copper ions. All solutions were deaerated by bubbling argon for 30 min before and during measurements.

Impedance measurements were performed under free corrosion potential, whereas potentiodynamic polarization curves were obtained at a scanning rate of 1 mV s^{-1}. The electrodes were immersed in the electrolyte and allowed to attain a steady value of free corrosion potential, which usually required ∼15 min in the absence of any additive and ∼25 min in the presence of either Cu^{2+} ions and/or BTAH. Unless otherwise indicated, impedance and polarization measurements were performed 0.5 h after the electrode had been immersed in the electrolyte.

Weight loss tests were carried out for 1 h in a 100 mL glass cell, thermostated at 30 ± 1 °C. Samples were in the form of circular disks of 1.5 cm diameter and 0.3 cm thickness.

Results and Discussion

Electrochemical Impedance Spectroscopy. Measurements were performed to determine the impedance parameters of the iron/electrolyte interface in the presence of various concentrations of Cu^{2+} and/or BTAH. Figure 1, panels A, B, and C, illustrate, respectively, the Nyquist, Bode, and phase angle plots

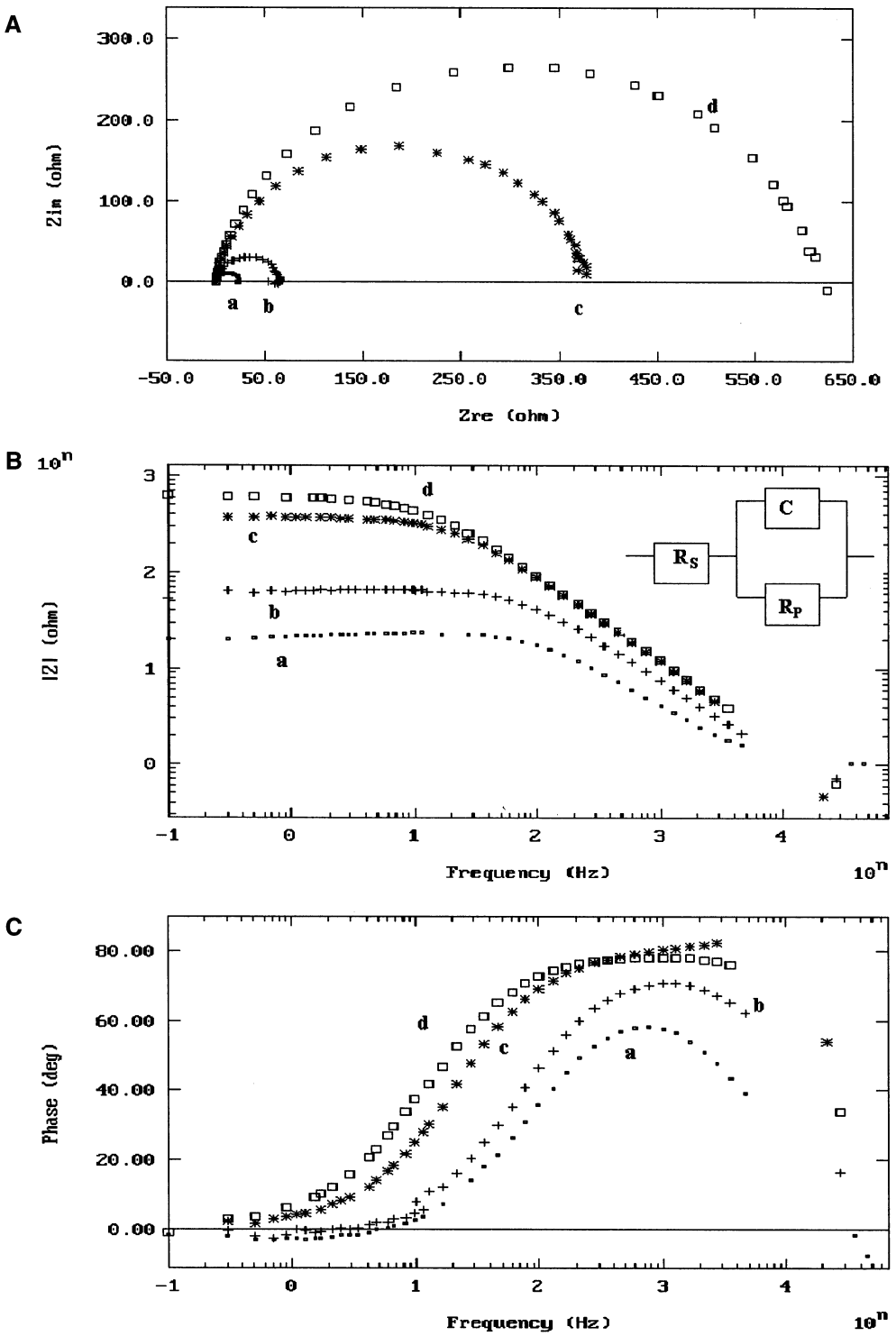

Figure 1. (A) Nyquist, (B) Bode and (C) phase angle plots of iron in 0.5 M H_2SO_4 in the presence of 5×10^{-3} M BTAH and different concentrations of Cu^{2+} ions: (a) 0, (b) 2×10^{-7}, (c) 10^{-6}, and (d) 5×10^{-6} M Cu^{2+} ions.

obtained on iron in the presence of various concentrations of Cu^{2+} ions added to a medium of 0.5 M H_2SO_4 inhibited by 5×10^{-3} M BTAH. These tests are marked **C** in Table 1. Increasing the concentration of copper ions from 2×10^{-7} to 5×10^{-6} M results in a significant increase in the size of the semicircle in Figure 1A, in the impedance of the interface in Figure 1B, and in the maximum phase angle in Figure 1C. The concentration of 5×10^{-6} M of Cu^{2+} ions was found to be a critical value above which further increase resulted in adverse effects, as shown below. The corresponding results obtained in the absence of BTAH under the same conditions of Cu^{2+} concentration are shown in Figure 2, panels A, B, and C (tests marked **A** in Table 1). They reveal only very modest changes in the above parameters, which are virtually negligible compared to the changes measured in the presence of BTAH (cf. Table 1, tests marked C).

Synergistic effects are also shown in the impedance spectra measured in the presence of the critical concentrations of Cu^{2+} ions (5×10^{-6} M) and various concentrations of BTAH (tests marked **D** in Table 1). The results are shown in Figure 3. An increase in the concentration of BTAH from 10^{-3} (curve c in Figure 3A) to 5×10^{-2} M (curve f in Figure 3A) leads to large

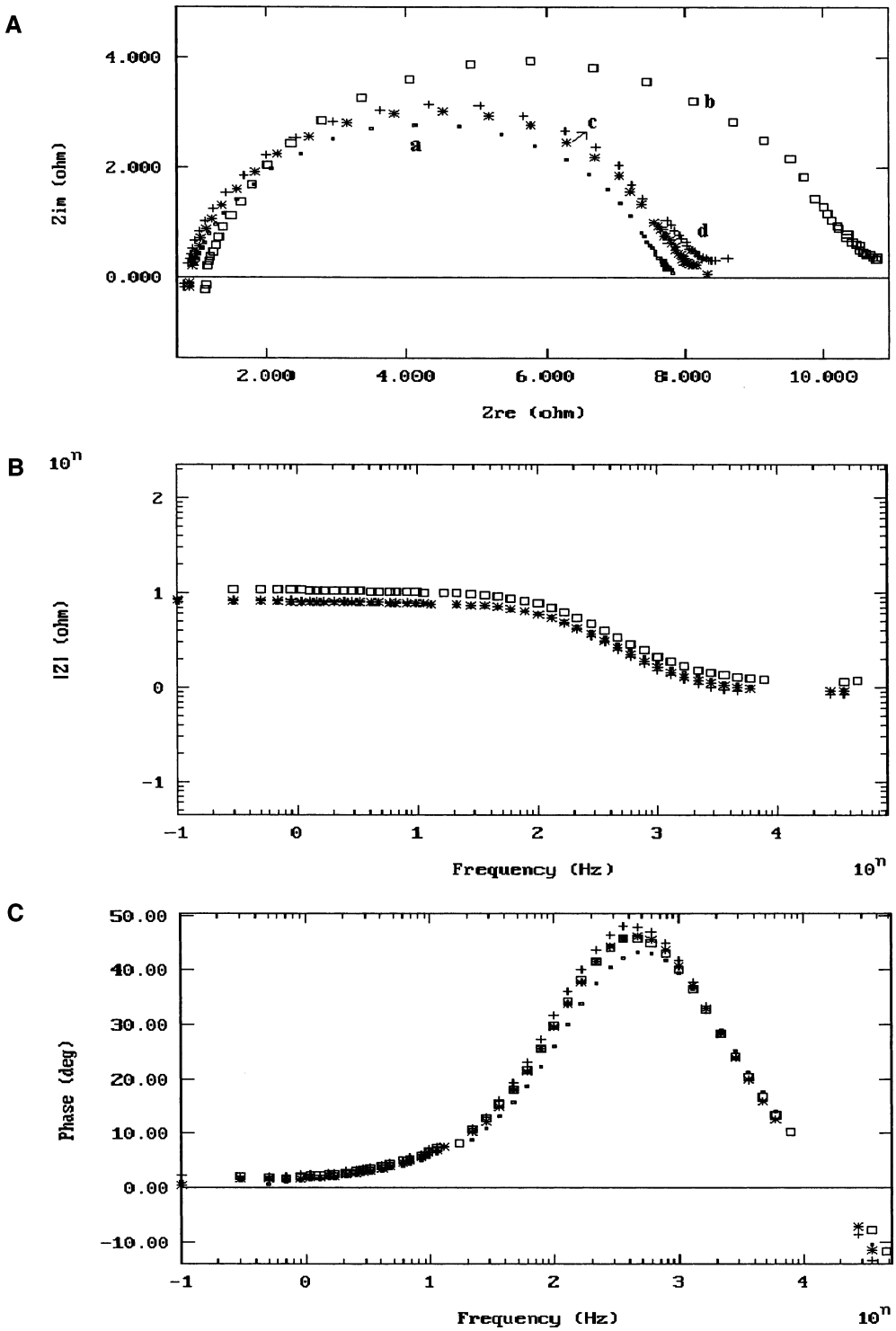

Figure 2. (A) Nyquist, (B) Bode and (C) phase angle plots of iron in 0.5 M H_2SO_4 (without BTAH) in the presence of different concentrations of Cu^{2+} ions: (a) 0, (b) 5×10^{-6}, (c) 10^{-5}, and (d) 10^{-4} M Cu^{2+} ions.

increases in the diameters of the semicircles in the Nyquist plot, in the impedance of the interface in the Bode plot, and in the maximum phase angle. These increases are much more substantial than those obtained in the absence of Cu^{2+} ions, which are shown in Figure 4, tests marked **B** in Table 1.

Equivalent Circuit. The simplest frame of reference for analyzing these data is the case of an ideal polarized electrode with the equivalent circuit shown in the inset of Figure 1B. The impedance of this circuit, Z, is composed of real (Z_{re}) and imaginary (Z_{im}) parts. It is related to the frequency of the signal, f, the polarization resistance, R_p, the double-layer capacity of the interface, C, and the resistance of the electrolyte, R_s, by[47]

$$Z = R_s + \frac{R_p}{1 + j2\pi fCR_p} \tag{7}$$

The double-layer capacitance of the interface is given by

$$C = (2\pi f_{max} R_p)^{-1} \tag{8}$$

where $j = \sqrt{-1}$ and f_{max} is the frequency corresponding to maximum phase angle in Figures 1C−4C. The polarization

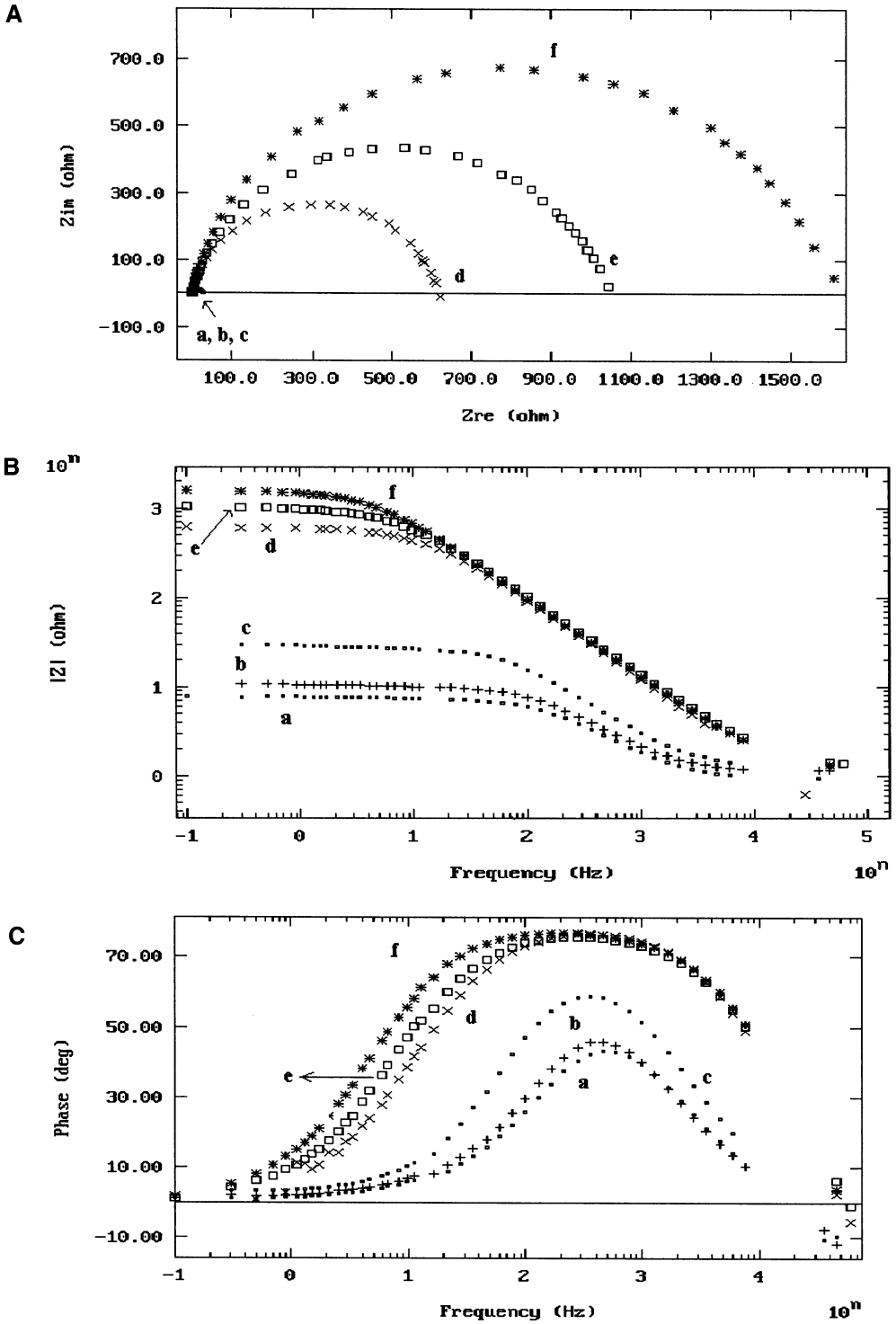

Figure 3. (A) Nyquist, (B) Bode and (C) phase angle plots of iron in a medium containing: (a) 0.5 M H_2SO_4, (b) 0.5 M H_2SO_4 + 5 × 10^{-6} M Cu^{2+} ions, (c) 0.5 M H_2SO_4 + 5 × 10^{-6} M Cu^{2+} ions + 10^{-3} M BTAH, (d) 0.5 M H_2SO_4 + 5 × 10^{-6} M Cu^{2+} ions + 5 × 10^{-3} M BTAH, (e) 0.5 M H_2SO_4 + 5 × 10^{-6} M Cu^{2+} ions + 10^{-2} M BTAH, and (f) 0.5 M H_2SO_4 + 5 × 10^{-6} M Cu^{2+} ions + 5 × 10^{-2} M BTAH.

resistance is related to the corrosion current, I_{corr}, by

$$I_{corr} = B/R_p \tag{9}$$

where B is a constant for each system.[48] Whereas the double-layer capacity is taken as a measure of the exposed (i.e., corroding) surface area, the polarization resistance is inversely proportional to the corrosion rate. Therefore, the presence of an efficient inhibitor decreases C and increases R_p compared to the values in the uninhibited medium. The increase in R_p is particularly useful in that it can be used to calculate the protection efficiency of the inhibitor, as shown below.

At the high-frequency limit (far right of Figures 1B and 2B), eq 7 predicts that the impedance of the interface, Z, approaches R_s, which is of the order of 1 ohm for this well-supported electrolyte. On the other hand, at the low-frequency limit (far left of Figures 1B and 2B) eq 7 predicts that Z approaches the sum of $R_s + R_p$. Under these conditions Z attains values that are orders of magnitude higher than R_s, and hence it is taken to

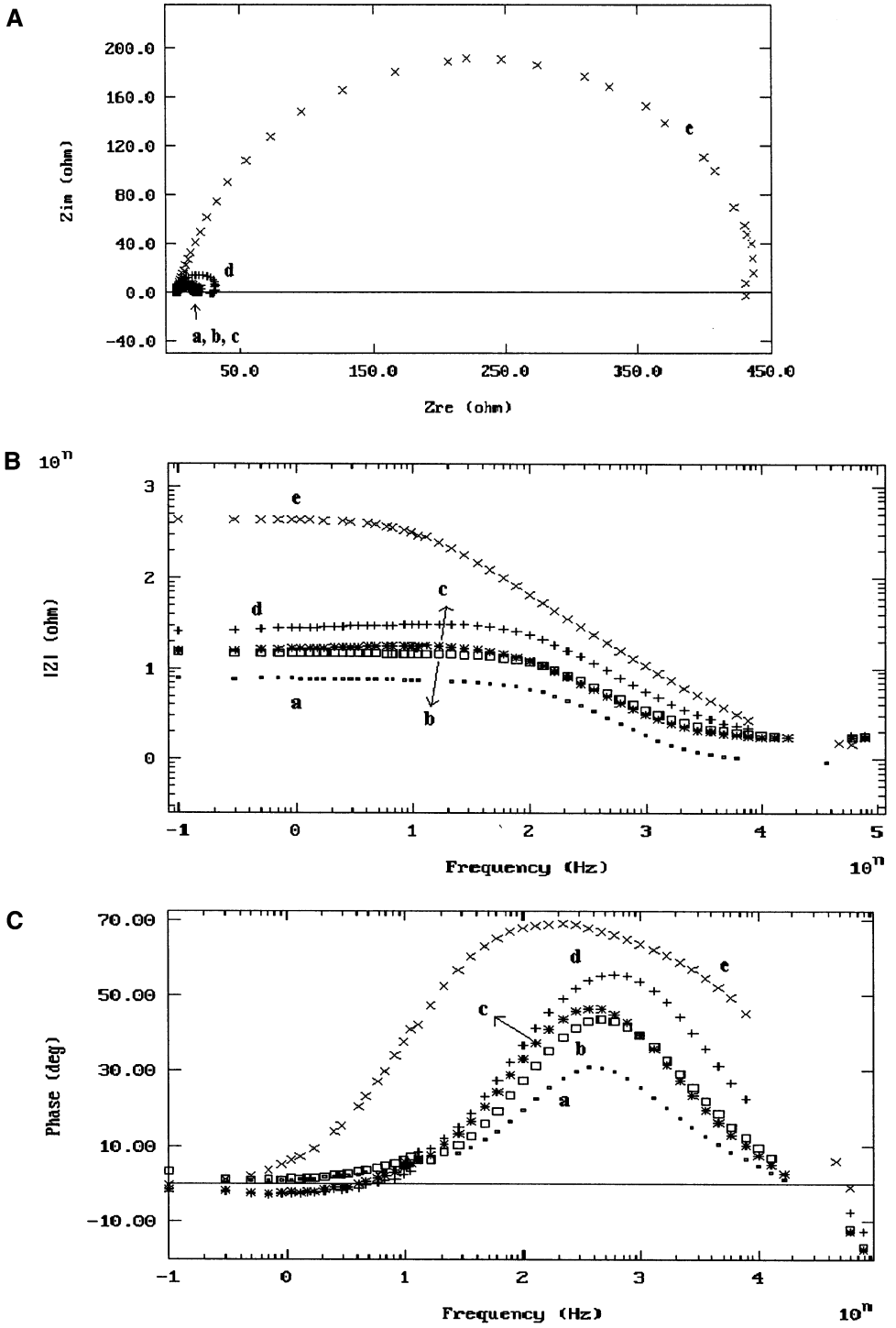

Figure 4. (A) Nyquist, (B) Bode and (C) phase angle plots of iron in 0.5 M H_2SO_4 (without Cu^{2+} ions) in the presence of different concentrations of BTAH: (a) 0, (b) 10^{-3}, (c) 5×10^{-3}, (d) 10^{-2}, and (e) 5×10^{-2} M BTAH.

be virtually equal to the polarization resistance, R_p. In the intermediate frequency range, the above simple model predicts a linear relation between log Z and log f with a slope of -1. The diameter of the semicircles in the Nyquist plots equals the polarization resistance of the interface.

Panels A−C of Figure 1 show that the increase in the concentration of Cu^{2+} ions, in the presence of 5×10^{-3} M BTAH, increases the polarization resistance of the interface, the slope of the log Z−log f straight line segment of the Bode plot (Figure 1B), and the maximum phase angle (Figure 1C), indicating that the system is approaching the case of an ideal polarized electrode, shown in the inset of Figure 1B. Furthermore, the magnitudes of those increases are much greater than those caused by the same concentrations of Cu^{2+} ions in the absence of BTAH, as shown in tests marked **A** in Table 1. The behavior of the system in 0.5 M H_2SO_4 shows a slope of -0.60, whereas in the same medium inhibited with 5×10^{-3} M BTAH $+ 5 \times 10^{-6}$M Cu^{2+} ions, it shows a slope of -0.88 in the region of intermediate frequency in Figure 1B. This approximates reasonably well the predictions of the model, particularly that we are using it as a basis for comparison of the effect of various additions of Cu^{2+} and BTAH on the impedance of the system. The values of the double-layer capacitance of the interface, C, were calculated from the results of the phase angle, like those

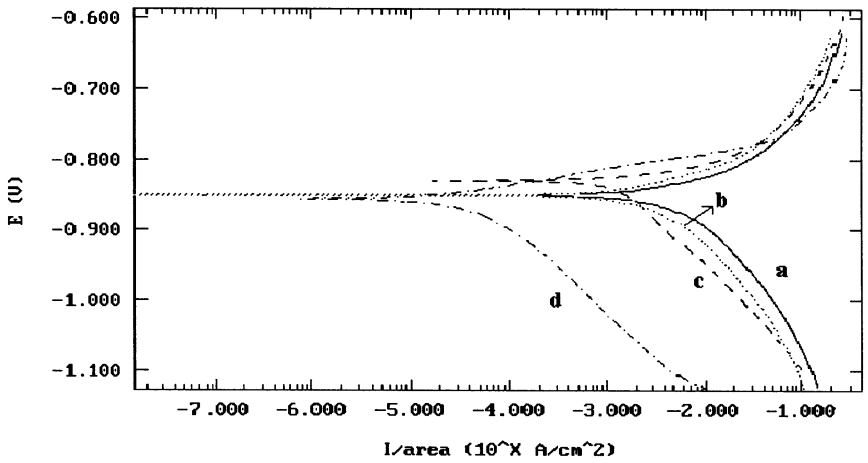

Figure 5. Polarization curves of iron in (a) 0.5 M H_2SO_4, (b) 0.5 M H_2SO_4 + 5 × 10^{-6} M Cu^{2+} ions, (c) 0.5 M H_2SO_4 + 5 × 10^{-3} M BTAH, and (d) 0.5 M H_2SO_4 + 5 × 10^{-6} M Cu^{2+} ions + 5 × 10^{-3}M BTAH.

shown in Figure 1C using eq 8. Table 1 lists the parameters calculated from the measured EIS diagrams obtained under various conditions.

In the absence of BTAH the increase in the concentration of Cu^{2+} ions has no significant effect on the polarization resistance, R_p, or on the double-layer capacitance, C, of the interface, as shown by the results of the tests marked **A** in Table 1. On the other hand, an increase in the concentration of BTAH, in the absence of Cu^{2+} ions, causes a significant increase in R_p and significant decreases in C, which is an illustration of the inhibiting efficiency of BTAH (see Figure 4 and the tests marked **B** in Table 1). The magnitude of the synergistic effect of BTAH and Cu^{2+} ions becomes evident upon comparison of the values of R_p and C produced by tests **A**, **B**, and **C** in Table 1. For example, a concentration of Cu^{2+} ions of 5 × 10^{-6} M (in the absence of BTAH) corresponds to values of R_p and C of 9.4 ohm cm^2 and 276.2 μF cm^{-2}, respectively, whereas a concentration of BTAH of 5 × 10^{-3} M (in the absence of Cu^{2+} ions) corresponds to an R_p of 16.5 ohm cm^2 and a C of 165.8 μF cm^{-2}. On the other hand, when the same medium is inhibited by a blend composed of 5 × 10^{-6} M Cu^{2+} ions and 5 × 10^{-3} M BTAH, one obtains R_p = 612.5 ohm cm^2 and C = 21.5 μF cm^{-2}. This remarkable increase in R_p, which is >1 order of magnitude above the values obtained in the presence of the best of the two additives, is an illustration of the synergistic effect of Cu^{2+} ions and BTAH. This effect is illustrated also in the polarization curves and the mass loss data shown below.

Protection Efficiency. A quantitative measure of the effect of a certain additive can be obtained by calculating the corrosion protection efficiency, which is given by

$$\% P = (1 - I_{corr(2)}/I_{corr(1)}) \times 100 = (1 - (R_{p(1)}/R_{p(2)})) \times 100 \quad (10)$$

where $I_{corr(1)}$ and $I_{corr(2)}$ are the corrosion current densities in the absence and in the presence of the inhibitor, respectively, and $R_{p(1)}$ and $R_{p(2)}$ are the corresponding polarization resistances. Table 1 lists the values of protection efficiency (% P) under various conditions. These values illustrate the synergistic effects of the Cu^{2+} ions and BTAH. For instance, a concentration of 5 × 10^{-6} M Cu^{2+} ions (in the absence of BTAH) corresponds to a value of % P of 28.72%. On the other hand, a concentration of 5 × 10^{-3} M BTAH (in the absence of Cu^{2+} ions) gives % P = 59.39%. However, in the presence of 5 × 10^{-6} M Cu^{2+} and 5 × 10^{-3} M BTAH, one obtains a value of % P of 98.91%. The same phenomenon is borne out by various other sets of numbers in Table 1. At a certain concentration of Cu^{2+} ions in the presence of BTAH, the % P is much greater than that obtained with the same concentration of BTAH in the absence of Cu^{2+} ions. This effect increases with the concentration of Cu^{2+} ions up to the critical concentration, as shown by the results of tests marked **C** in Table 1. An increase in the concentration of BTAH at a certain concentration of Cu^{2+} ions causes a monotonic increase in the efficiency.

Polarization Curves and Weight Loss. The synergistic effects of Cu^{2+} and BTAH in inhibiting the corrosion of iron are also evident in the potentiodynamic polarization curves shown in Figure 5. The upper and lower parts refer to the anodic and cathodic partial reactions, eq 5 and 6, respectively. The presence of 5 × 10^{-6} M Cu^{2+} ions (in the absence of BTAH) (curve b) has only a small retarding effect on the rate of the cathodic partial reaction (eq 6), whereas a concentration of 5 × 10^{-3} M BTAH (in the absence of Cu^{2+} ions) (curve c) has a moderate retarding effect. On the other hand, the simultaneous presence of both Cu^{2+} ions and BTAH at the above levels (curve d) shows a >1 order of magnitude decrease in the rate of the cathodic partial reaction (eq 6) over a broad range of potentials compared to that obtained in their absence (curve a) or in the presence of either one of them (curves b and c). The inhibiting efficiency % P can also be calculated from the cathodic currents using eq 10. Using the results of Figure 5, at −1.0 V, one obtains values of % P of 33.90% in the presence of 5 × 10^{-6} M Cu^{2+} ions (in the absence of BTAH), 51.58% in the presence of 5 × 10^{-3} M BTAH (in the absence of Cu^{2+} ions), and 98.57% in the presence of both Cu^{2+} ions and BTAH at the same levels. The latter value is comparable to the value of 98.91% calculated at the free corrosion potential, as given in Table 1. Note that the effects on the rate of the anodic partial reaction (eq 5) are much less pronounced. This evidence indicates that the blend acts as an efficient cathodic inhibitor for the corrosion of iron in H_2SO_4. Similar effects are shown in Figure 6, which was measured in the presence of a higher concentration (10^{-5} M) of Cu^{2+} ions. Figures 7 and 8 illustrate, respectively, the effects

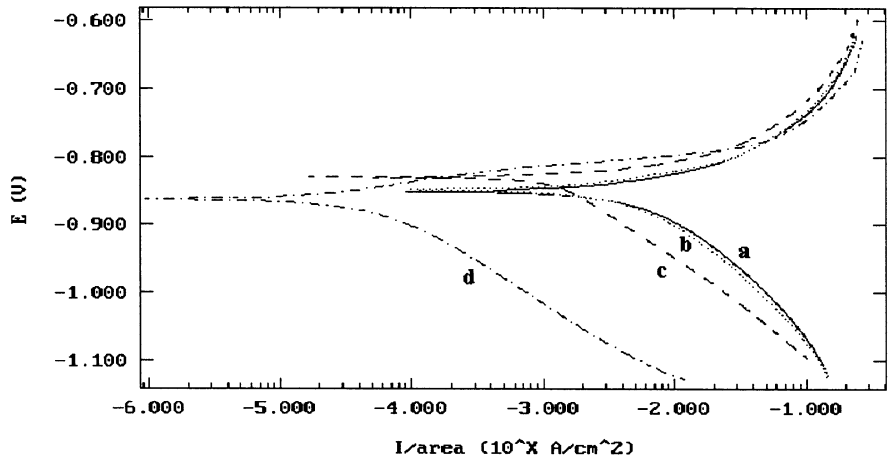

Figure 6. Polarization curves of iron in (a) 0.5 M H_2SO_4, (b) 0.5 M H_2SO_4 + 10^{-5} M Cu^{2+}, (c) 0.5 M H_2SO_4 + 5×10^{-3} M BTAH, and (d) 0.5 M H_2SO_4 + 10^{-5} M Cu^{2+} ions + 5×10^{-3}M BTAH.

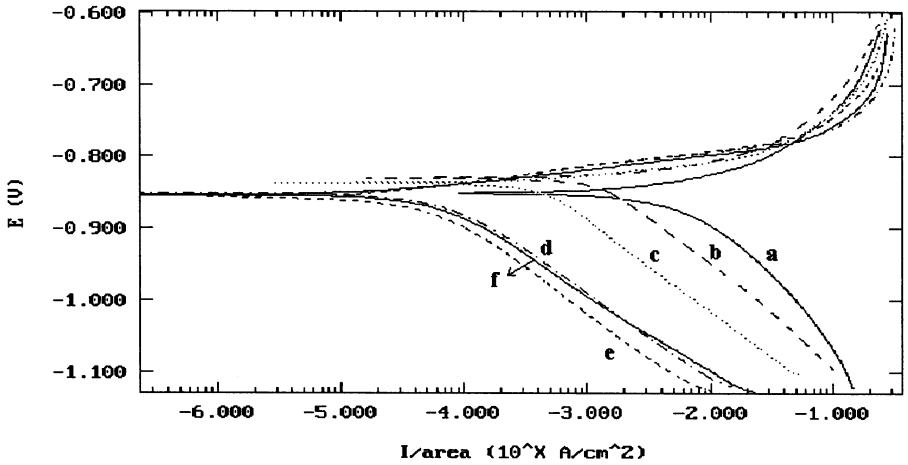

Figure 7. Polarization curves of iron in 0.5 M H_2SO_4 in the presence of 5×10^{-3} M BTAH with different concentrations of Cu^{2+} ions: (a) 0.5 M H_2SO_4, (b) 0.5 M H_2SO_4 + 5×10^{-3} M BTAH, (c) 0.5 M H_2SO_4 + 5×10^{-3} M BTAH + 2×10^{-7} M Cu^{2+} ions, (d) 0.5 M H_2SO_4 + 5×10^{-3} M BTAH + 10^{-6} M Cu^{2+} ions, (e) 0.5 M H_2SO_4 + 5×10^{-3} M BTAH + 5×10^{-6} M Cu^{2+} ions, and (f) 0.5 M H_2SO_4 + 5×10^{-3} M BTAH + 10^{-5} M Cu^{2+} ions.

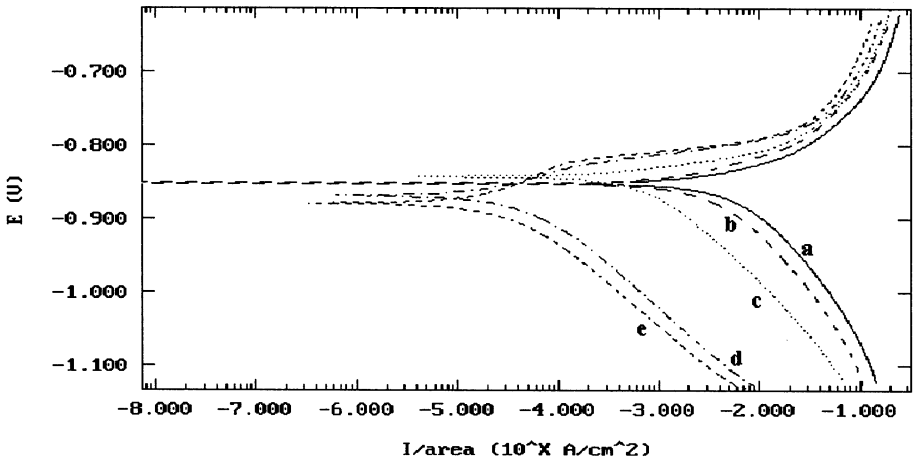

Figure 8. Polarization curves of iron in 0.5 M H_2SO_4 in the presence of 5×10^{-6} M of Cu^{2+} ions with different concentrations of BTAH: (a) 0.5 M H_2SO_4, (b) 0.5 M H_2SO_4 + 5×10^{-6} M Cu^{2+} ions, (c) 0.5 M H_2SO_4 + 5×10^{-6} M Cu^{2+} ions + 10^{-3} M BTAH, (d) 0.5 M H_2SO_4 + 5×10^{-6} M Cu^{2+} ions + 5×10^{-3} M BTAH, and (e) 0.5 M H_2SO_4 + 5×10^{-6} M Cu^{2+} ions + 10^{-2} M BTAH.

of increasing the concentration of Cu^{2+} (at a constant concentration of BTAH) and of BTAH (at a constant concentration of Cu^{2+} ions) on the polarization curves of iron in 0.5 M H_2SO_4.

The synergistic effects are also evident in the results of the weight loss tests that are listed in Table 2. In the presence of 5×10^{-3} M BTAH (in the absence of Cu^{2+} ions) there is a significant reduction in the corrosion rate with a protection efficiency of 78.31%. On the other hand, in the presence of 5×10^{-6} M of Cu^{2+} ions and 5×10^{-3} M BTAH the % P increases to 98.22%. This is a further illustration of the

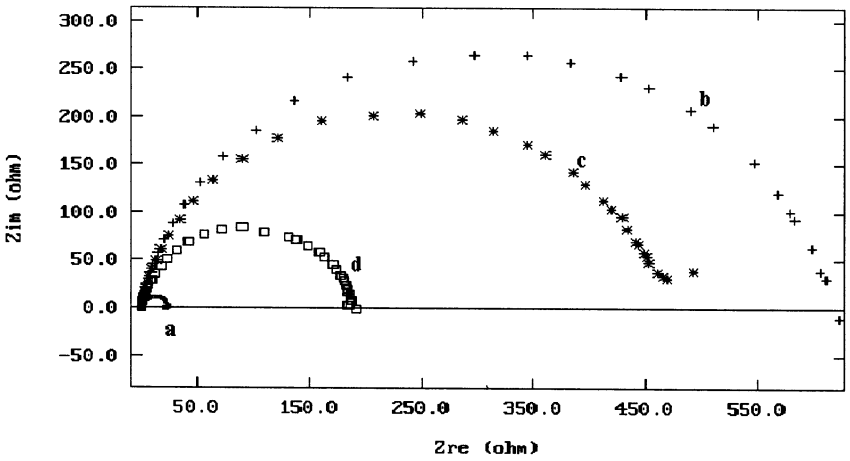

Figure 9. Nyquist plots of iron in 0.5 M H_2SO_4 in the presence of 5×10^{-3} M BTAH with different concentrations of Cu^{2+} ions: (a) 0, (b) 5×10^{-6}, (c) 10^{-5}, and (d) 10^{-4} M Cu^{2+}.

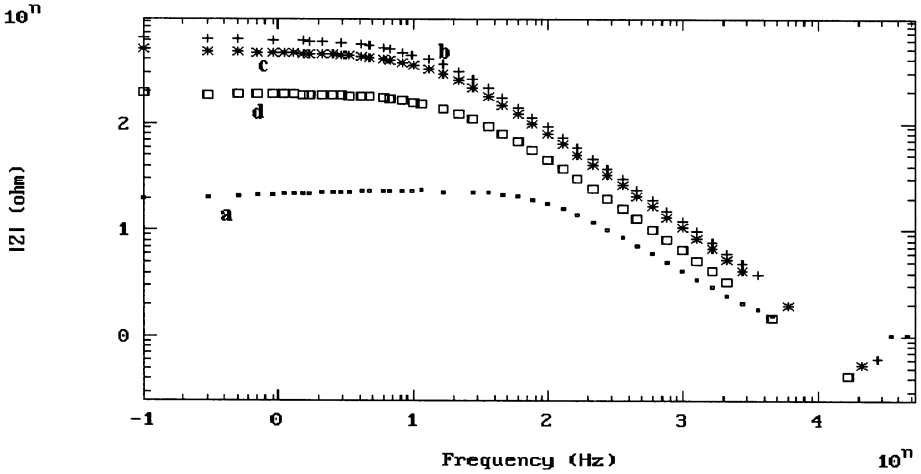

Figure 10. Bode plots of iron in 0.5 M H_2SO_4 in the presence of 5×10^{-3} M BTAH with different concentrations of Cu^{2+} ions: (a) 0, (b) 5×10^{-6}, (c) 10^{-5}, and (d) 10^{-4} M Cu^{2+}.

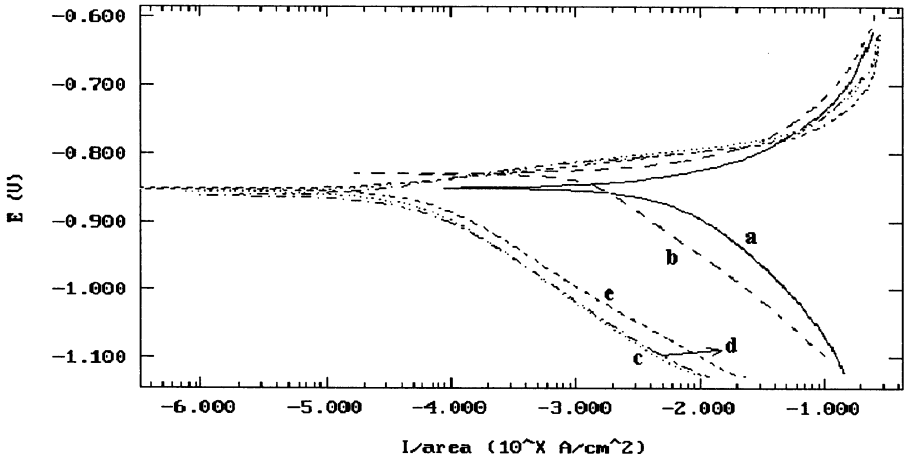

Figure 11. Polarization curves of iron in 0.5 M H_2SO_4 in the presence of 5×10^{-3} M BTAH with different concentrations of Cu^{2+} ions: (a) 0.5 M H_2SO_4, (b) 0.5 M $H_2SO_4 + 5 \times 10^{-3}$ M BTAH, (c) 0.5 M $H_2SO_4 + 5 \times 10^{-3}$ M BTAH $+ 5 \times 10^{-6}$ M Cu^{2+} ions, (d) 0.5 M $H_2SO_4 + 5 \times 10^{-3}$ M BTAH $+ 10^{-5}$M Cu^{2+} ions, and (e) 0.5 M $H_2SO_4 + 5 \times 10^{-3}$ M BTAH $+ 10^{-4}$ M Cu^{2+} ions.

synergistic effects exhibited above by the results of the EIS experiments.

Film Formation. The free corrosion potential of iron in the acidic medium is about −850 mV versus (Hg/Hg_2SO_4), which is equivalent to about −235 mV versus (SHE) at 30 °C. This is a fairly cathodic value that is sufficient to reduce Cu^{2+} to metallic copper. The reaction is known to proceed in two consecutive steps,[49,50] that is

$$Cu^{2+} + e \leftrightarrow Cu^{+} \quad \text{slow} \tag{11}$$

$$Cu^{+} + e \leftrightarrow Cu^{0} \quad \text{fast} \tag{12}$$

The formation of Cu^{+} ions on an iron surface on which BTAH

TABLE 2: Corrosion Rates (CR) of Iron and Protection Efficiencies in 0.5 M H_2SO_4 Inhibited by 5×10^{-3} M BTAH in the Presence of Different Concentrations of Copper Ions

electrolytic composition	CR, mg cm^{-2} h^{-1}	% *P*
0.5 M H_2SO_4	7.207	
$+ 5 \times 10^{-3}$ M BTAH	1.563	78.31
$+ 1 \times 10^{-4}$ M Cu^{2+}	0.385	94.65
$+ 1 \times 10^{-5}$	0.205	79.16
$+ 5 \times 10^{-6}$	0.128	98.22

is adsorbed favors the formation of the Cu(I)BTA complex,[42,49] that is

$$Cu^{2+}_{(aq)} + e \rightarrow Cu^{+}_{(ads)} \quad (13)$$

$$Cu^{+}_{(ads)} + BTAH_{(ads)} = Cu(I)BTA_{(ads)} + H^{+} \quad (14)$$

One can safely argue that the lifetime of a free Cu^+ ion will be shortened by the presence of the adsorbed BTAH such that we can justifiably write eq 14.

G. R. Gutz[51] et al. showed that Cu^{2+} ions are reduced to copper(I) and accumulated as the Cu(I)BTA complex on a hanging mercury drop electrode at 0.0V versus SCE, which is equivalent to 0.241 V versus NHE. The formation of Cu(I)-BTA was also reported in several papers dealing with the electrodeposition of Cu on a gold substrate, wherein the authors[49,52] showed that the presence of benzotriazole yields a smoother deposit compared to that obtained from additive-free solutions. They attributed this effect to the formation of a Cu-(I)BTA complex at the interface, which makes it less favorable for the cuprous ions to diffuse freely on the surface. In principle, this complex can also polymerize, that is

$$n\text{Cu(I)BTA} = [\text{Cu(I)BTA}]_n \quad (15)$$

The present results are compatible with eq 14 in that an increase in the concentration of BTAH or copper ions (up to 5×10^{-6} M) shifts this equilibrium toward the right, that is, to the formation of the Cu(I)BTA complex.

Adverse Effect. It was shown above that the protection efficiency increases (due to synergistic effects) as the concentration of Cu^{2+} ions increases up to 5×10^{-6} M in the presence of 5×10^{-3} M BTAH. Beyond this critical concentration, a further increase in the concentration of Cu^{2+} ions increases the double-layer capacity and decreases the polarization resistance of the interface and, hence, the protection efficiency decreases. The magnitude of this adverse effect increases with the concentration of Cu^{2+} ions as shown in Figures 9 and 10 and in the results of tests **D**, **E**, and **F** in Table 1. This may be attributed to the excessive deposition of Cu^{2+} ions as Cu atoms on the iron surface, which were clearly visible on the iron surface after tests in the presence of higher concentrations ($\sim 10^{-4}$ M) of Cu^{2+} ions. This freshly deposited copper is a better catalyst for the h.e.r. (eq 6), which is the rds of the corrosion reaction. Hence, the presence of this metallic copper promotes the rds and consequently promotes also the overall corrosion reaction. This interpretation is substantiated by the polarization curves in Figure 11. The increase in the concentration of Cu^{2+} ions beyond the critical concentration increases the rate of the hydrogen evolution reaction (eq 6) beyond the value produced by the critical concentration.

Summary

The present work reveals that benzotriazole, which shows only a modest protection efficiency against the acid corrosion of iron, can be made to exhibit very high protection efficiency via a synergistic effect with micromolar amounts of Cu^{2+} ions. This synergistic effect appears also in the double-layer capacity (which is a measure of the exposed area) and the polarization resistance of the interface, in the polarization curves of the electrode, and in the corrosion rate of iron in the media containing both BTAH and Cu^{2+} ions. It is attributed to the formation of a protective Cu(I)BTA complex on the iron surface that inhibits the cathodic partial reaction (eq 6). The film forms as a result of the reduction of Cu^{2+} to Cu^+ ions, which react with the adsorbed BTAH to form the complex. An optimum concentration of 5×10^{-6} M has been identified for a BTAH concentration of 5×10^{-3} M. Further increase in the Cu^{2+} concentration decreased the magnitude of the synergistic effect. This was attributed to the excessive deposition of metallic copper on the electrode surface. This freshly deposited copper promotes the cathodic partial reaction (eq 6), which is the rate-determining step of the overall corrosion reaction.

References and Notes

(1) Dugdale, I.; Cotton, J. B. *Corros. Sci.* **1963**, *3*, 69.
(2) Cotton, J. B.; Scholes, I. R. *Br. Corros. J.* **1967**, *2*, 1.
(3) Walsh, J. F.; Dhariwal, H. S.; Gutierrez-Sosa, A.; Finetti, P.; Muryn, C. A.; Brookes, N. B.; Oldman, R. J.; Thornton, G. *Surf. Sci.* **1998**, *415*, 423.
(4) Metikos-Hukovic, M.; Babic, R.; Marinovic, A. *J. Electrochem. Soc.* **1998**, *145*, 4045.
(5) Babic, R.; Metikos-Hukovic, M. *Thin Solid Films* **2000**, *359*, 88.
(6) Hegazy, H. S.; Ashour, E. A.; Ateya, B. G. *J. Appl. Electrochem.* **2001**, *31*, 1261.
(7) da Costa, S. L. F. A.; Agostinho, S. M. L.; Nobe, K. *J. Electrochem. Soc.* **1993**, *140*, 3483.
(8) Alkire, R.; Cangellari, A. *J. Electrochem. Soc.* **1989**, *136*, 913.
(9) Maciel, J. M.; Agostinho, S. M. L. *J. Appl. Electrochem.* **2000**, *30*, 981.
(10) Huyanh, N.; Bottle, S. E.; Notoya, T.; Schweinsberg, D. P. *Corros. Sci.* **2000**, *42*, 259.
(11) Aramaki, K. *Corros. Sci.* **2001**, *43*, 1985.
(12) Fenelon, A. M.; Breslin, C. B. *J. Appl. Electrochem.* **2001**, *31*, 509.
(13) Jinturkar, P.; Guan, Y. C.; Han, K. N. *Corrosion* **1998**, *54*, 106.
(14) Chung, E.-H.; Nobe, K. Presented at the 193rd Meeting of the Electrochemical Society, Inc., San Diego, CA, May 3−8, 1998.
(15) Brusic, V.; Frankel, G. S.; Schrott, A. G.; Petersen, T. A. *J. Electrochem. Soc.* **1993**, *140*, 2507.
(16) Cao, P. G.; Yao, J. L.; Zheng, J. W.; Gu, R. A.; Tian, Z. Q. *Langmuir* **2002**, *18*, 100.
(17) Sathianandhan, B.; Balakarishnan, K.; Subramanyan, N. *Br. Corros. J.* **1970**, *5*, 270.
(18) Rodrigues, P. R. P.; De Andrade, A. H. P.; Agostinho, S. M. L. *Br. Corros. J.* **1967**, *16*, 169.
(19) Devasenapathi, A.; Raja, V. S. *J. Mater. Sci.* **1998**, *33*, 3345.
(20) Nobe, K.; Chin, R. J. *J. Electrochem. Soc.* **1971**, *118*, 545.
(21) Eldakar, N.; Nobe, K. *Corrosion* **1981**, *36*, 271.
(22) Eldakar, N.; Nobe, K. *Corrosion* **1977**, *33*, 129.
(23) Eldakar, N.; Nobe, K. *Corrosion* **1976**, *32*, 238.
(24) Gomma, G. K. *Mater. Chem. Phys.* **1998**, *55*, 235.
(25) Lewis, G. *Br. Corros. J.* **1981**, *16*, 169.
(26) Thierry, D.; Leygraf, C. *J. Electrochem. Soc.* **1985**, *132*, 1009.
(27) Mansfeld, F.; Smith, T.; Parry, E. T. *Corrosion* **1971**, *27*, 289.
(28) Yeung, H.; Chan, H.; Weaver, M. J. *Langmuir* **1999**, *15*, 3348.
(29) Vogt, M. R.; Polewska, W.; Magnussen, O. M.; Behm, R. J. *J. Electrochem. Soc.* **1997**, *144*, L113.
(30) Tornkvist, C.; Thierry, D.; Bergman, J.; Liedberg, B.; Leygraf, C. *J. Electrochem. Soc.* **1989**, *136*, 58.
(31) Vogt, M. R.; Nichols, R. J.; Magnussen, O. M.; Behm, R. J. *J. Phys. Chem. B* **1998**, *102*, 5859. Polewska, W.; Vogt, M. R.; Magnussen, O. M.; Behm, R. J. *J. Phys. Chem. B* **1999**, *103*, 10440.
(32) Cho, K.; Kishimoto, J.; Hashizume, T.; Pickering, H. W.; Sakurai, T. *Appl. Surf. Sci.* **1995**, *87/88*, 380.
(33) Cho, K.; Kishimoto, J.; Hashizume, T.; Sakurai, T. *Jpn. J. Appl. Phys.* **1994**, *33*, L125.
(34) Fang, B. S.; Olson, C. G.; Lynch, D. W. *Surf. Sci.* **1986**, *176*, 476.
(35) Poling, G. W. *Corros. Sci.* **1970**, *10*, 359.
(36) Youda, R.; Nishihara, H.; Aramaki, K. *Corros. Sci.* **1988**, *28*, 87.

(37) Nilsson, J.-O.; Tornkvist, C.; Liedberg, B. *Appl. Surf. Sci*. **1989**, *37*, 306.
(38) Tromans, D.; Sun, R. *J. Electrochem. Soc*. **1991**, *138*, 3235.
(39) Modestov, A. D.; Zhou, G. D.; Wu, Y. P.; Notoya, T.; Schweinsberg, D. P. *Corros. Sci*. **1994**, *36*, 1931.
(40) Tromans, D. *J. Electrochem. Soc*. **1998**, *145*, L 42.
(41) Kester, J. J.; Furtak, T. E.; Bevolo, A. J. *J. Electrochem. Soc.* **1982**, *129*, 1716.
(42) Rubim, J.; Gutz, I. G. R.; Sala, C.; Orville-Thomas, J. *J. Mol. Struct*. **1983**, *100*, 571.
(43) Youda, R.; Nishihara, H.; Aramaki, K. *Electrochim. Acta* **1990**, *35*, 1011.
(44) Brusic, V.; Frisch, M. A.; Eldridge, B. N.; Novak, F. P.; Kaufman, F. B.; Rush, B. M.; Frankel, G. S. *J. Electrochem. Soc*. **1991**, *138*, 2253.
(45) Abd Elhamid, M. H.; Ateya, B. G.; Pickering, H. W. Presented at the 193rd Meeting of the Electrochemical Society, Inc., San Diego, CA, May 3−8, 1998.
(46) Gomma, G. K. *Mater. Chem. Phys.* **1998**, *55*, 131.
(47) Mansfeld, F.; Shih, H.; Green, H.; Tsai, C. H. *Electrochemical Impedance: Analysis and Interpretation*; ASTM STP 1188; American Society for Testing and Materials: Philadelphia, PA, 1993; p 37.
(48) Stern, M.; Geary, A. L. *J. Electrochem. Soc*. **1957**, *104*, 56.
(49) Becky Leung, T. Y.; Kang, M.; Corry, B. F.; Gewirth, A. A. *J. Electrochem. Soc.* **2000**, *147*, 3326.
(50) Scendo, M.; Malyszko, J. *J. Electrochem. Soc*. **2000**, *147*, 1758.
(51) Nacimento, V. B.; Gutz, I. G. R. *Electrochim. Acta* **1998**, *43*, 2423.
(52) Schmidt, W. U.; Alkire, R. C.; Gewirth, A. A. *J. Electrochem. Soc.* **1996**, *143*, 3122.